Inorganic Chemistry

ARTICLE

pubs.acs.org/IC

Temperature-Dependent Exchange Interaction in Molecular Magnets $Cu(hfac)_2L^R$ Studied by EPR: Methodology and Interpretations

Sergey L. Veber,*[,†] Matvey V. Fedin,[†] Ksenia Yu. Maryunina,[†] Alexey Potapov,[‡] Daniella Goldfarb,[‡] Edward Reijerse,[§] Wolfgang Lubitz,[§] Renad Z. Sagdeev,[†] Victor I. Ovcharenko,[†] and Elena G. Bagryanskaya[†]

[†]International Tomography Center SB RAS, 630090 Novosibirsk, Russia

[‡]Department of Chemical Physics, The Weizmann Institute of Science, 76100 Rehovot, Israel

[§]Max-Planck-Institut für Bioanorganische Chemie, 45470 Mülheim/Ruhr, Germany

ABSTRACT: Exchange-coupled spin triads nitroxide−copper(II)−nitroxide are the key building blocks of molecular magnets $Cu(hfac)_2L^R$. These compounds exhibit thermally induced structural rearrangements and spin transitions, where the exchange interaction between spins of copper(II) ion and nitroxide radicals changes typically by 1 order of magnitude. We have shown previously that electron paramagnetic resonance (EPR) spectroscopy is sensitive to the observed magnetic anomalies and provides information on both inter- and intracluster exchange interactions. The value of intracluster exchange interaction is temperature-dependent ($J(T)$), that can be accessed by monitoring the effective g-factor of the spin triad as a function of temperature ($g_{eff}(T)$). This paper describes approaches for studying the $g_{eff}(T)$ and $J(T)$ dependences and establishes correlations between them. The experimentally obtained $g_{eff}(T)$ dependences are interpreted using three different models for the mechanism of structural rearrangements on the molecular level leading to different meanings of the $J(T)$ function. The contributions from these mechanisms and their manifestations in X-ray, magnetic susceptibility and EPR data are discussed.

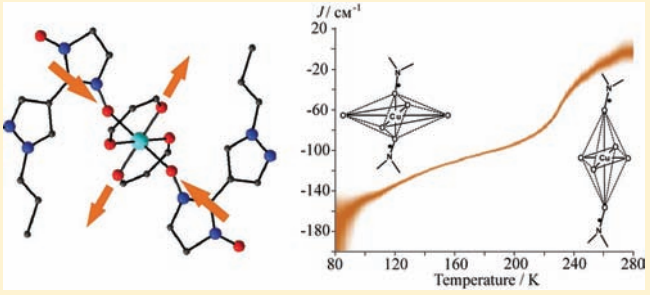

INTRODUCTION

Switchable molecule-based magnetic materials are actively studied in the field of molecular magnetism. In most cases their ability to switch between two or several magnetic states is due to the effects of thermally induced or light-induced spin crossover or valence tautomerism.[1−14] Recently, similar phenomena have been found for the new family of molecular magnets $Cu(hfac)_2L^R$ later called "breathing crystals". These compounds have a polymer-chain structure containing copper hexafluoroacetylacetonates ($Cu(hfac)_2$) and pyrazolyl-substituted nitronylnitroxides (L^R) with different substituents (Scheme 1).

Breathing crystals do not contain any spin-crossover metals, but still exhibit pronounced thermally induced and light-induced magnetic anomalies due to the structural rearrangements in exchange-coupled heterospin clusters of copper(II) with nitronylnitroxides. During these reversible rearrangements the unit cell volume changes by up to 15% (crystals "breathe") and the effective magnetic moment significantly varies, reflecting electron pairing in the heterospin clusters.[15−21] Structural changes accompanied by magnetic anomalies have also been found for several other copper(II) based compounds.[22−28]

The exchange interactions in compounds of the $Cu(hfac)_2L^R$ family and their changes by temperature or light can conveniently be studied using EPR spectroscopy.[29−37] In particular, the intracluster exchange interaction (J) between the copper(II) ion and the nitroxide radical can be evaluated through the analysis of the temperature-dependent effective g-factor (g_{eff}) of the spin triad nitroxide−copper(II)−nitroxide, which is the main EPR parameter characterizing the structural rearrangements in $Cu(hfac)_2L^R$. Our previous work has shown that the intracluster exchange coupling J changes by about 1 order of magnitude with temperature inducing transitions between weakly coupled ($|J| \ll kT$) and strongly coupled ($|J| \gg kT$) spin states.[31] Along with the studies of strong intracluster exchange (ca. 100−200 cm^{-1}), EPR allows for investigating the intercluster exchange interactions which are much smaller compared to J (ca. 1−10 cm^{-1}).[36] Interestingly, the intercluster interaction occurs between neighboring polymer chains; i.e., the apparent magnetic chains spread across structural polymer chains.

Information on the magnitude and temperature dependence of the intracluster exchange interaction is crucial for establishing the magnetostructural correlations in breathing crystals and optimization of their magnetic properties. Using one of the complexes ($Cu(hfac)_2L^{Bu}\cdot 0.5C_8H_{18}$) we previously obtained the temperature dependence of intracluster exchange $J(T)$ based on the experimentally measured dependence of the effective g-factor of the spin triad $g_{eff}(T)$.[32] However, the systematic EPR study of the dependences of $g_{eff}(T)$ and $J(T)$ for several compounds and various experimental settings (e.g., microwave

Received: June 2, 2011
Published: September 22, 2011

dx.doi.org/10.1021/ic2011869 | *Inorg. Chem.* 2011, 50, 10204–10212

Scheme 1. (a) Chemical Structure of L^R and $Cu(hfac)_2$ and (b) Polymer Chain of $Cu(hfac)_2L^{Pr}$. [a]

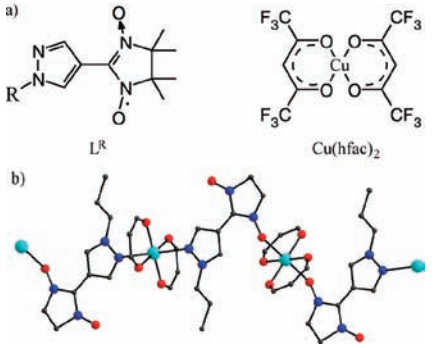

[a] Cu, light blue ball; O, red ball; C, black ball; N, blue ball. The hydrogen atoms, the geminal methyl groups of L, and the trifluoromethyl groups of the hfac ligands are omitted for clarity.

frequency band, single crystal vs powder sample choice, etc.) was not yet done. In this work we address these important questions. We again chose the compounds with gradual spin transitions ($Cu(hfac)_2L^{Pr}$ and $Cu(hfac)_2L^{Bu}\cdot 0.5C_8H_{18}$) that gave us an opportunity to investigate the temperature dynamics of the structural and magnetic parameters in detail. Moreover, the gradual character of the changes in this type of compounds raises several additional questions of interest. To date, the main manifestations of structural rearrangements and spin transitions in breathing crystals were characterized in detail using X-ray analysis, SQUID magnetometry, and EPR. However, the mechanism of the structural rearrangements in octahedral CuO_6 units on the molecular level still remains unclear, especially in the case of gradual phase transitions. When a gradual phase transition is observed, the X-ray data show that the elongated (Jahn−Teller) axis in the CuO_6 units gradually shortens with temperature, while the other axis simultaneously lengthens. In this way the two axes are interchanged during the transition. Both the magnetic susceptibility dependence ($\mu_{eff}(T)$) and the EPR data confirm the gradual character of this change. On the other hand, it is well established that only the elongated octahedral conformations are usually stable for copper(II) ions;[38] therefore, gradual dependences may result from spatial or temporal averaging. As will be shown below, EPR studies of $g_{eff}(T)$ and $J(T)$ functions during gradual phase transitions allowed us to shed some light onto this complicated question.

The paper is structured in the following way. After description of experimental details and brief introduction to the general trends of EPR of breathing crystals, we describe the methodology of $J(T)$ measurement. The approaches of using polycrystalline or single crystal samples with their pros and cons are discussed, and the $J(T)$ functions for two selected compounds are experimentally obtained. The gradual shape of these functions leads us to the following discussion on possible interpretations of this graduality. We propose three models of structural rearrangements on the molecular level and discuss them in the light of previously known structural and magnetic data on breathing crystals and other Jahn−Teller systems.

EXPERIMENTAL SECTION

Two compounds of the breathing crystals family, $Cu(hfac)_2L^{Pr}$ and $Cu(hfac)_2L^{Bu}\cdot 0.5C_8H_{18}$ (Pr = propyl, Bu = butyl, C_8H_{18} = octane),

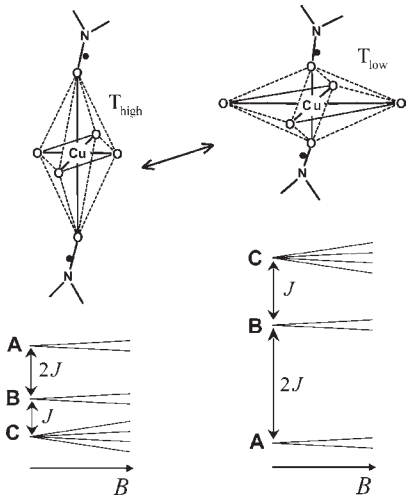

Figure 1. Schematic drawing of thermally induced structural changes in the CuO_6 octahedron and theoretically expected energy levels of the spin triad.

have been synthesized according to previously developed procedures.[15,19] Their structure and magnetic susceptibility behavior were also investigated previously.[15,19] Although a number of compounds of the breathing crystals family exhibit thermal hysteresis, in the systems studied here it is not observed. EPR measurements at Q-band ($\nu_{mw} \approx 34$ GHz) were carried out in continuous-wave (CW) mode using a commercial Bruker Elexsys E580 X/Q-band EPR spectrometer and a Bruker ER200D continuous wave Q-band EPR spectrometer, both equipped with an Oxford Instruments temperature control system ($T = 4-300$ K). EPR measurements at W-band ($\nu_{mw} = 94.9$ GHz) were carried out using a home-built EPR spectrometer[39] in CW-mode. We used both polycrystalline powders and single crystals of the studied compounds in different experiments.

RESULTS AND DISCUSSION

General Consideration. Molecular magnets $Cu(hfac)_2L^R$ with "head-to-head" motif contain two types of paramagnetic species in their polymer-chain structure: the one-spin paramagnetic center >N−Cu−*N*< in a CuO_4N_2 unit (later called "isolated copper(II) ion") and the symmetric nitroxide−copper(II)−nitroxide cluster >N−$^{\bullet}$O−Cu−O$^{\bullet}$−*N*< in a CuO_6 unit (later called "three-spin cluster" or "spin triad"). As was already mentioned, lowering of the temperature leads to shortening of two Cu−O_L bonds in the CuO_6 unit and simultaneous lengthening of two Cu−O_{hfac} bonds, where the subscripts L and hfac refer to the nitroxide and hfac oxygens, respectively (Figure 1). Thus, at different temperatures equatorial or axial coordination of nitroxide radical to copper(II) ion is stabilized resulting in a different sign and value of the intracluster exchange interaction.[26]

Both powder and single crystal EPR spectra show signals of the isolated copper(II) ion and the strongly temperature-dependent signals of the spin triads (Figure 2). The spin-Hamiltonian of the symmetric exchange-coupled nitroxide−copper(II)−nitroxide spin triad can be written in the following form

$$\hat{H} = \beta \mathbf{B}\mathbf{g}^{R}(\mathbf{S}^{R1} + \mathbf{S}^{R2}) + \beta \mathbf{B}\mathbf{g}^{Cu}\mathbf{S}^{Cu} - 2J(\mathbf{S}^{R1} + \mathbf{S}^{R2})\mathbf{S}^{Cu} - 2J'\mathbf{S}^{R1}\mathbf{S}^{R2} \quad (1)$$

where the superscripts R1 and R2 correspond to the two nitroxides and Cu to the copper(II) ion, $\mathbf{g}^R$ and $\mathbf{g}^{Cu}$ are the

dx.doi.org/10.1021/ic2011869 |Inorg. Chem. 2011, 50, 10204–10212

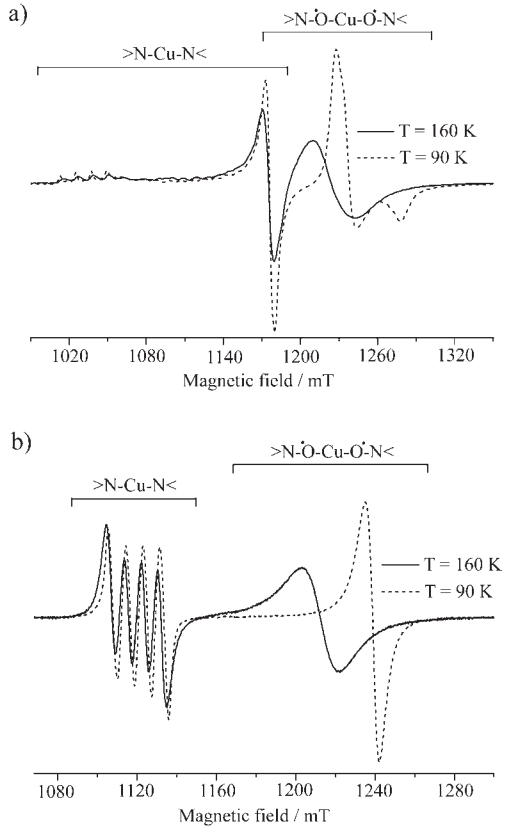

Figure 2. EPR spectra of $Cu(hfac)_2L^{Pr}$ at temperatures 90 and 160 K measured in Q-band ($\nu_{mw} \approx 34$ GHz): (a) polycrystalline powder and (b) single crystal (arbitrary orientation).

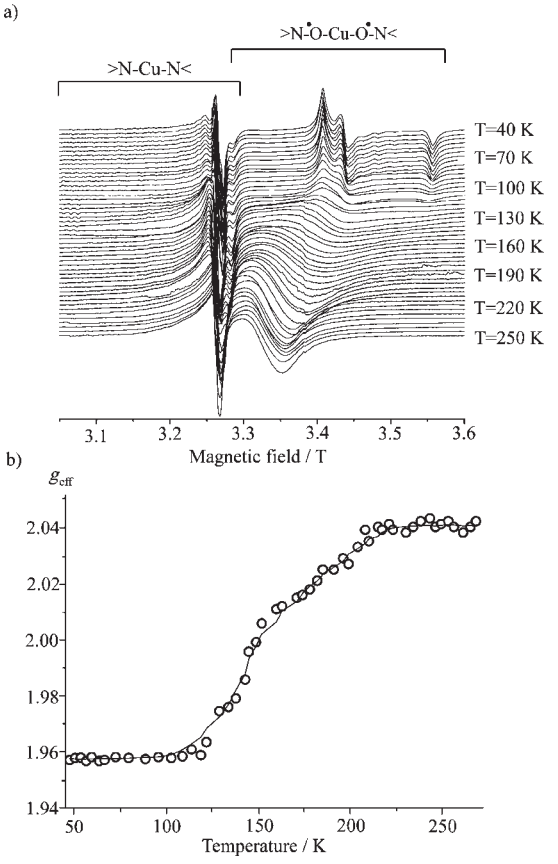

Figure 3. (a) Temperature-dependent EPR spectra of a $Cu(hfac)_2L^{Pr}$ powder sample measured in W-band ($\nu_{mw} = 94.9$ GHz) and (b) effective g-factor of the spin triad vs temperature calculated from powder EPR spectra as a gravity center of the spectrum of a triad.

corresponding **g**-tensors. The nitroxides are assumed to be equivalent. Anisotropy of nitroxide g-factor is negligible in comparison with copper(II) ion anisotropy, and thus, the isotropic g-factor g^R is assumed, i.e., $\mathbf{g}^R = g^R\hat{\mathbf{1}}$, where $\hat{\mathbf{1}}$ is the unity matrix. $\mathbf{B} = [0, 0, B]$ is the magnetic field along the z-axis, J corresponds to the exchange interaction between copper(II) and each nitroxide, and J' corresponds to the exchange interaction between nitroxides ($J < 0$ corresponds to the antiferromagnetic coupling).

The last term in the spin-Hamiltonian (eq 1) can be neglected since for symmetric linear spin triads $|J| \gg |J'|$.[40] Another good approximation for breathing crystals is $|J| \gg B$;[31,41] therefore, the effective **g**-tensors of multiplets of spin triad are given by eqs 2:[42]

$$\mathbf{g}^A = (4g^R\hat{\mathbf{1}} - \mathbf{g}^{Cu})/3 \qquad \mathbf{g}^B = \mathbf{g}^{Cu}$$
$$\mathbf{g}^C = (2g^R\hat{\mathbf{1}} + \mathbf{g}^{Cu})/3 \qquad (2)$$

The ratio between the exchange interaction J and the thermal energy kT determines the shape of the EPR spectrum of the spin triad. At low temperatures (typically 50−70 K) only the signals of the lower multiplet A are observed, since $kT \ll |J|$, $J < 0$.[31] At intermediate and high temperatures $kT \geq |J|$ and multiplets B and C become also populated. However, in most cases one cannot observe resolved EPR lines of multiplets A, B, and C, but a single averaged line in the temperature-dependent center of gravity of the spectrum. This can be explained by fast mixing (10^9−10^{12} s^{-1}) between different multiplets of the individual spin triad[35] and by intercluster exchange interaction between spin triads of neighboring polymer chains.[36] The position (i.e., effective g-factor $g_{eff}(T)$) of the line of the spin triad changes during the phase transition and is the main spectroscopic measure of structural rearrangements and spin transitions available by EPR. Experimentally, two different approaches to obtain the $g_{eff}(T)$ dependence can be considered: the use of polycrystalline powder samples or of single crystals. As will be shown below, both approaches are useful; however, the use of single crystals is superior and therefore will be discussed in more detail.

Measurement of $g_{eff}(T)$ Using Polycrystalline Powder Samples. The use of polycrystalline powder samples for EPR studies of breathing crystals is in principle more convenient, as it does not require growing of crystals of sufficient size and adjusting their orientation toward the magnetic field in the spectrometer. However, two experimental complications have to be overcome.

The first complication concerns the overlap of signals of the spin triad and the isolated copper(II) ion at high temperature. Figure 3a shows the temperature-dependent powder spectra of $Cu(hfac)_2L^{Pr}$ measured in W-band (ν_{mw} = 94.9 GHz). The $g_{\|}$ component of the isolated copper(II) ion that appears at magnetic fields $B \sim 2.8$−2.9 T was not recorded due to the limitation of the field sweep amplitude, but the $g_{\perp}$ component was observed at $B \sim 3.27$ T. Although we used a high microwave frequency, still the undesired overlap at high temperatures was unavoidable. One would expect that a further increase of the mw frequency may solve the problem; however, in this case the second complication appears caused by the finite mixing rates between different multiplets of spin triad.

dx.doi.org/10.1021/ic2011869 |Inorg. Chem. 2011, 50, 10204–10212

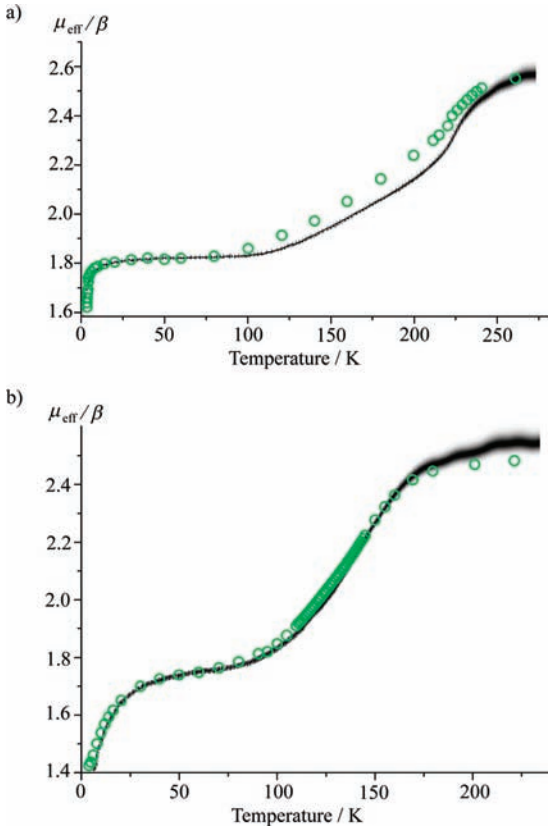

Figure 4. Experimental (green) $\mu_{eff}(T)$ dependences and calculation (black) using the obtained $J(T)$ functions for (a) $Cu(hfac)_2L^{Pr}$ and (b) $Cu(hfac)_2L^{Bu}\cdot 0.5C_8H_{18}$ compounds.

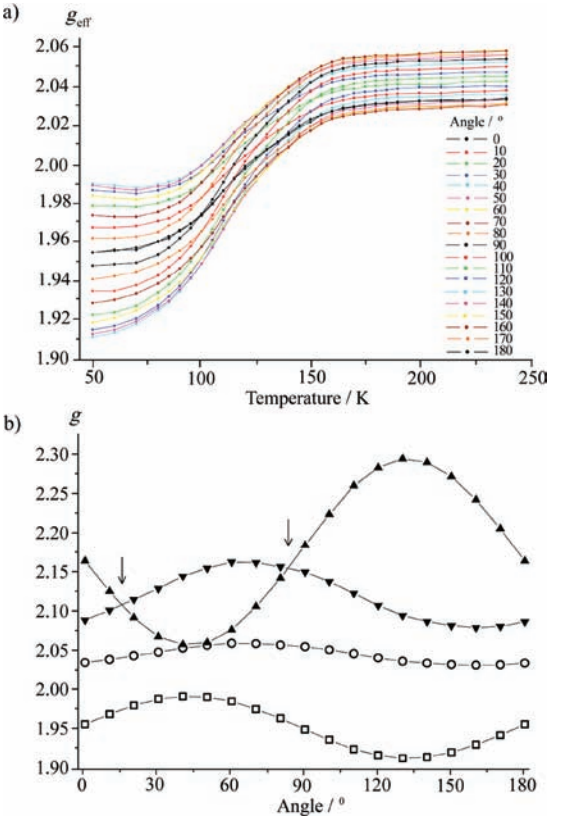

Figure 5. (a) Temperature dependence of g_{eff} obtained in Q-band ($\nu_{mw} \approx 34$ GHz) for a $Cu(hfac)_2L^{Bu}\cdot 0.5C_8H_{18}$ single crystal fixed in the sample holder (arbitrary orientation) and rotated in the range 0−180° around the sample holder axis. (b) Angular dependence of g_{eff} at 240 K (○) and 50K (□), and corresponding (▼,▲) g-factor of the copper(II) ion calculated using equations $g^{Cu} = 3g^C - 2g^R$ and $g^{Cu} = 4g^R - 3g^A$ at 240 and 50 K, respectively. Arrows show the orientations for which the g-factor of the copper(II) ion is the same at low (50 K) and high (240 K) temperature.

As we have shown in ref 35 the mixing rates between different multiplets of the spin triad cannot be considered fast at high EPR frequencies; e.g., this is the case for $Cu(hfac)_2L^{Pr}$ already at 122 GHz. When mixing rates lay in the intermediate exchange region, instead of the average EPR line of multiplets A, B, and C, a complicated pattern is detected. In order to calculate the effective g-factor of this pattern one should use numerical simulations that involve many unknowns such as electron relaxation rates, etc.

Thus, the trade-off between sufficient spectral resolution, sensitivity, and simple approach for $g_{eff}(T)$ measurement is not easy. Nevertheless, we obtained a meaningful dependence $g_{eff}(T)$ (Figure 3b), the shape of which reasonably agrees with the $\mu_{eff}(T)$ dependence (Figure 4a). But, as we will show below, a superior approach is provided by using oriented single crystals.

Measurement of $g_{eff}(T)$ Using Single Crystals. The use of single crystals has the advantage of higher sensitivity and does not suffer from the overlap between EPR lines of the spin triads and isolated copper(II) ions (Figure 2b); therefore, there is no need for high-frequency experiments where the fast exchange condition in the triads may be violated. Moreover, the EPR signal of the three-spin cluster in the case of a single crystal is a symmetric line whose g-factor can easily and reliably be obtained in the whole temperature range. However, the following factor needs to be taken into account. We already mentioned that during the structural rearrangements in the octahedral CuO_6 units containing spin triads the elongated axis changes its direction (Figure 1); therefore, the components of the $\mathbf{g}$-tensor of copper(II) $\mathbf{g}^{Cu}$ change as well. The mean g-value does not change significantly during this transformation; thus, for powder measurements, this complication is not essential, but for single crystals, where a certain orientation is chosen for $g_{eff}(T)$ measurement, it is crucial.

Figure 5a shows the $g_{eff}(T)$ dependences obtained in Q-band for a single crystal of $Cu(hfac)_2L^{Bu}\cdot 0.5C_8H_{18}$ at different orientations with respect to the magnetic field. The crystal was fixed in the sample holder (arbitrary orientation) and then rotated in the range 0−180° around the sample holder axis.

The dependences $g_{eff}(T)$ measured at different angles are pronouncedly different. Similar to the magnetic susceptibility, the $g_{eff}(T)$ dependences have two plateaus at the high and low temperature limits yielding the g^{Cu} values at these temperatures. The low-temperature plateau ($kT \ll |J|$) implies that only the lowest multiplet A with $g^A = (4g^R - g^{Cu})/3$ is populated, i.e., $g_{eff} = g^A$, and thus g^{Cu} can easily be found (using the value $g^R \approx 2.007$[30]). At the high-temperature plateau ($kT \gg |J|$) the gravity center corresponds to $g^C = (2g^R + g^{Cu})/3$,[31] i.e., $g_{eff} = g^C$, and the value g^{Cu} can again be found. As was expected, the obtained values g^{Cu} do not coincide at high- and low-temperature plateaus, because the components of $\mathbf{g}^{Cu}$ tensor interchange due to the flip of the Jahn−Teller axis in the CuO_6 octahedron (Figure 5b).

Of course, the dependence $\mathbf{g}^{Cu}(T)$ is unknown, and therefore, it would be desirable to find the proper orientation where $g^{Cu}(T) =$ const. This indeed can be done by rotating the crystal at low- and

dx.doi.org/10.1021/ic2011869 |Inorg. Chem. 2011, 50, 10204–10212

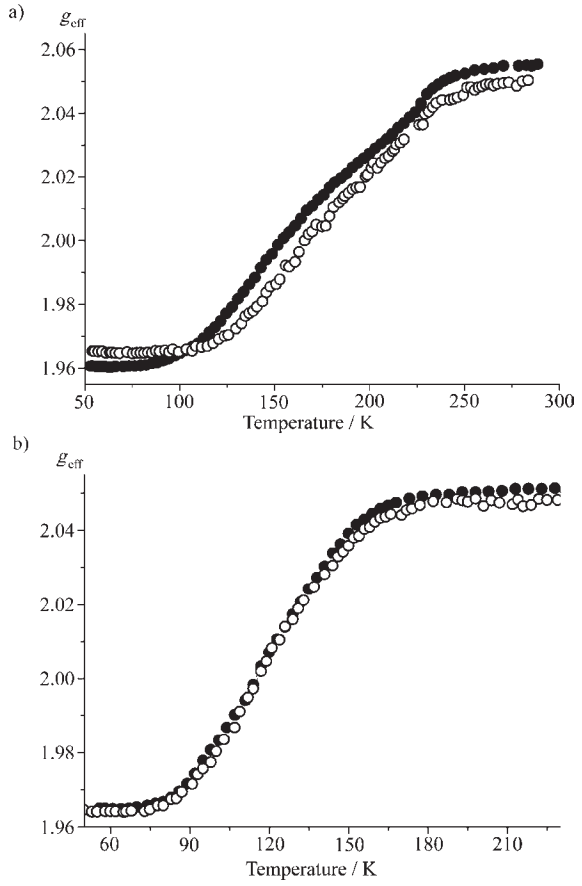

Figure 6. $g_{eff}(T)$ dependences obtained from Q-band (●) and W-band (○) EPR spectra for the single crystals of (a) $Cu(hfac)_2L^{Pr}$ and (b) $Cu(hfac)_2L^{Bu}\cdot 0.5C_8H_{18}$ compounds. Selected orientations of single crystals toward the magnetic field satisfy $g^{Cu}(T) \approx$ const criterion.

high-temperatures (where the corresponding plateaus are reached) and calculating the observed g^{Cu} at each orientation. The crossings of angular dependences are shown in Figure 5b (marked by arrows) and correspond to the desired orientations where $g^{Cu}(T) \approx$ const. We cannot test the fulfillment of condition $g^{Cu}(T) =$ const experimentally at the intermediate temperatures (between the plateaus), but there is no reason to expect significant deviations from it. As soon as the proper orientation is found, the $g_{eff}(T)$ dependence with $g^{Cu}(T) \approx$ const can be measured. Note that it seems straightforward to choose the crystal orientation with the magnetic field along the $O_{hfac}-Cu-O_{hfac}$ axis that does not flip during the structural rearrangement (and hence $g^{Cu} \approx$ const (Figure 1)). However, we did not succeed with this approach, because the polymer chains containing CuO_6 units also exhibit structural changes with temperature, so that the whole octahedrons slightly rotate with respect to the magnetic field. Therefore, the above-described procedure of finding the correct orientations of the crystal where $g^{Cu}(T) \approx$ const (Figure 5b) is superior, and all $g_{eff}(T)$ dependences shown below were obtained in this way.

It is instructive to investigate the $g_{eff}(T)$ function versus the mw frequency band. Figure 6a shows the $g_{eff}(T)$ dependences for $Cu(hfac)_2L^{Pr}$ obtained from Q- and W-band data. The obtained $g_{eff}(T)$ functions are significantly different. The $g_{eff}(T)$ function obtained at Q-band starts to grow at $T \approx 80$ K in agreement with $\mu_{eff}(T)$,[31] since at this temperature the upper multiplets B and C of the spin triad start to populate. At the same time, the $g_{eff}(T)$ function obtained at W-band starts to grow only at $T \approx 120$ K. The reason for the observed difference is that mixing rates cannot be considered infinitely fast at W-band for $Cu(hfac)_2L^{Pr}$, in agreement with our previous work,[35] and the observed signal is not a correct average over the three multiplets of a triad. For the other compound, $Cu(hfac)_2L^{Bu}\cdot 0.5C_8H_{18}$, the $g_{eff}(T)$ dependences obtained from Q- and W-band data perfectly coincide (Figure 6b). Again, this agrees well with our previous observation that the mixing rates for this compound are fast at EPR frequencies up to 244 GHz.[35] Thus, it is important to choose the appropriate mw frequency band. As was outlined in ref 35, the straightforward criterion for fast mixing is that the width of the EPR line of a triad must change monotonically with temperature: this is the case for $Cu(hfac)_2L^{Bu}\cdot 0.5C_8H_{18}$ at Q /W-bands and for $Cu(hfac)_2L^{Pr}$ at Q-band, and is not the case for $Cu(hfac)_2L^{Pr}$ at W-band. Therefore, in the following sections we analyze $g_{eff}(T)$ dependences obtained in Q-band.

Interpretation of the $g_{eff}(T)$ Dependence and Information on the Exchange Interaction. Spin transitions in the family of breathing crystals and their manifestations are very diverse. In many compounds the spin transition is abrupt, i.e., $\mu_{eff}(T)$, $g_{eff}(T)$, and distances in the octahedron CuO_6 change abruptly in a narrow temperature range. Compounds with abrupt spin transitions are most requested for potential applications; however, deeper insight into the origin and mechanisms of these magnetic anomalies can be obtained from studying compounds with gradual spin transitions, as is done in this work. At the same time, the gradual character of the observed structural rearrangements and $g_{eff}(T)$ dependences raises several questions on the interpretation of these values.

Below we propose and discuss three possible models explaining the observed structural and magnetic phenomena in breathing crystals. The intracluster exchange interaction was characterized in a framework of each model using experimentally obtained $g_{eff}(T)$ dependences.

Model A: Gradual Structural Changes in Octahedral Units CuO_6. Magnetic susceptibility dependences $\mu_{eff}(T)$, X-ray data,[15,19] and EPR data ($g_{eff}(T)$) all report gradual changes for the compounds of the breathing crystals family studied in this work. Therefore, it would be quite natural to assume that indeed the structural and magnetic properties of the CuO_6 units containing spin triads change gradually. In this model, all spin triads have the same geometry that changes with temperature and causes changes of interspin distances and electron orbitals and, consequently, of the intracluster exchange interaction J. The $g_{eff}(T)$ dependences measured in this paper satisfy conditions of fast mixing rates allowing us to use the analytical expression 3 for their interpretation.[31]

$$\mathbf{g}_{eff}(T) = \frac{\mathbf{g}^A + \mathbf{g}^B\cdot e^{2J/kT} + 10\cdot\mathbf{g}^C\cdot e^{3J/kT}}{1 + e^{2J/kT} + 10e^{3J/kT}} = \frac{(4\mathbf{g}^R - \mathbf{g}^{Cu}) + 3\mathbf{g}^{Cu}\cdot e^{2J/kT} + 10\cdot(2\mathbf{g}^R + \mathbf{g}^{Cu})\cdot e^{3J/kT}}{3(1 + e^{2J/kT} + 10e^{3J/kT})} \quad (3)$$

Here, $g^R \approx 2.007$ and g^{Cu} can be measured as described above. The unknown to be determined by fitting of the experimental $g_{eff}(T)$ dependence is the intracluster exchange interaction $J(T)$.

Figure 7 shows the $J(T)$ distribution for both studied compounds which fit well the experimental $g_{eff}(T)$ dependences measured for single crystals at Q-band (Figure 6). Both $J(T)$

dx.doi.org/10.1021/ic2011869 |Inorg. Chem. 2011, 50, 10204–10212

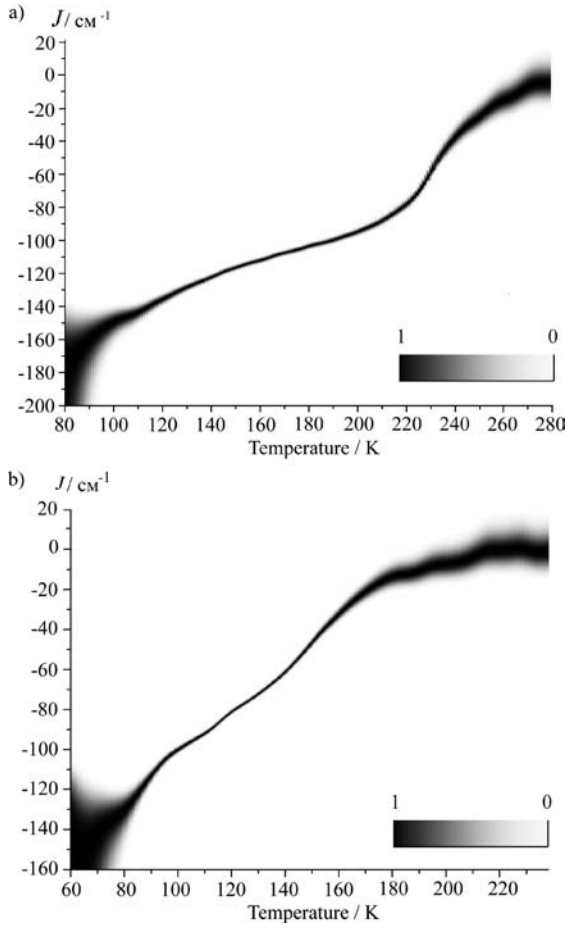

Figure 7. Temperature dependence of exchange interaction $J(T)$ of (a) $Cu(hfac)_2L^{Pr}$ and (b) $Cu(hfac)_2L^{Bu}\cdot 0.5C_8H_{18}$ calculated using the experimental function $g_{eff}(T)$ and eq 3. Normalized probability of the exchange interaction value J in the range 1 to 0 is shown. The error of the experimental determination of the g-factor (± 0.0005) was taken into account during the fitting procedure and determines the width of the calculated $J(T)$ distribution at intermediate temperatures.

curves show a strong dependence of intracluster exchange interaction on temperature. The shapes of the curves are notably different, in agreement with different shapes of $\mu_{eff}(T)$ dependences shown in Figure 4. At high and medium temperatures the J value can be determined quite precisely due to the strong dependence of g_{eff} on J. At low temperature only the lowest multiplet is populated, and therefore, only the limits for J can be set.

To check the reliability of obtained $J(T)$ functions we used them in the calculation of corresponding $\mu_{eff}(T)$ dependences:

$$\mu_{eff}^2 = 0.5\mu_{tr,eff}^2 + 0.5\mu_{is,eff}^2 = \frac{3(g^A)^2 + 3(g^B)^2\cdot e^{2J/kT} + 30(g^C)^2\cdot e^{3J/kT}}{8(1 + e^{2J/kT} + 2e^{3J/kT})} + 0.5\mu_{is,eff}^2 \quad (4)$$

Here, subscripts "tr" and "is" correspond to the spin triad and the isolated copper(II) ion, respectively.[31] The decrease of the effective magnetic moment at temperatures $T < 50$ K is caused by intercluster exchange interaction[36] (J_{Int}) which was taken into account as described elsewhere[32,43] ($J_{Int} = -1.5$ cm^{-1} and $J_{Int} = -12$ cm^{-1} for $Cu(hfac)_2L^{Pr}$ and $Cu(hfac)_2L^{Bu}\cdot 0.5C_8H_{18}$, respectively). Figure 4 shows that the $J(T)$ functions obtained from EPR describe the $\mu_{eff}(T)$ dependences reasonably well for both compounds; thus, the validity of these functions is additionally confirmed.

In the discussed model the obtained $J(T)$ functions have literal meanings; i.e., the exchange interaction in every spin triad changes gradually with temperature. This implies a gradual elongation and shortening of corresponding bonds in the CuO_6 octahedrons. However, it is widely accepted in the literature[44−46] that due to the Jahn−Teller effect the only stable conformation of copper(II) octahedrons is the elongated geometry (one axis is noticeably longer than the two others), and the flip of the elongated axis has a jumplike character. Moreover, some of our EPR data also indicate the weak points of the discussed model. An inherent property of eq 3 is that when the following eq 5 is fulfilled, g_{eff} becomes independent of g^{Cu} and equal to g^R.

$$10e^{3J/kT} + 3e^{2J/kT} - 1 = 0 \quad (5)$$

The solution of eq 5 gives $J/kT \approx -0.97$. Consequently, the described situation when $g_{eff} = g^R$ does not depend on g^{Cu} should take place for both studied compounds, because (i) g_{eff} changes from $g_{eff} > 2$ to $g_{eff} < 2$ and thus the value $g_{eff} = 2 \approx g^R$ is necessarily met during the phase transition, and (ii) $|J|/kT$ changes from $|J|/kT \ll 1$ to $|J|/kT \gg 1$ ($J < 0$)[31] and thus $J/kT \approx -0.97$ is also necessarily found during the phase transition. This means that independently of the crystal orientation and the dependence $g^{Cu}(T)$, all curves $g_{eff}(T)$ shown in Figure 5a must converge at one point $g_{eff} = g^R$. However, this prediction of eq 3 was never observed experimentally. One of the explanations could be that in this model A the obtained exchange interactions are effective values and should be considered as temporal or/and spatial averages of the exact molecular-level ones, as we will discuss below.

Model B: Vibrational Averaging Due to the Dynamic Jahn−Teller Effect. Despite the stability of the elongated geometry, in a number of copper(II) complexes the flattened geometries were detected by both X-ray and EPR.[47] An exhaustive study of these compounds (including EXAFS) demonstrated that the observed flattened geometry is a result of fast vibrational averaging between two elongated geometries due to the dynamic Jahn−Teller effect. Typical jump frequencies between the elongated geometries can reach 10^9 s^{-1} and higher leading to the observation of isotropic-like EPR spectra at X- and Q-bands.[48]

X-ray studies of breathing crystals exhibiting gradual spin transitions show that flattened geometries of CuO_6 octahedrons are observed at certain ranges of intermediate temperatures for all compounds studied so far.[15,19] Taking into account the flexibility of the geometry of the CuO_6 units that allows for structural rearrangements to occur, this observation seems to be consistent with manifestations of dynamic Jahn−Teller effects observed previously.

In this model B during a gradual phase transition fast jumps between high- and low-temperature (HT, LT) geometries occur, so that X-ray, EPR, and magnetic susceptibility data reflect values averaged in time. At the low and high temperature limits the CuO_6 octahedrons are permanently in LT and HT geometries in agreement with $\mu_{eff}(T)$ and $g_{eff}(T)$ plateaus. However, at intermediate temperatures the mean residence probabilities at HT and LT geometries vary yielding the corresponding dependences

dx.doi.org/10.1021/ic2011869 |Inorg. Chem. 2011, 50, 10204–10212

of the observed parameters. In this case the experimental $g_{eff}(T)$ dependence can be described by the following equation

$$g_{eff}(T) = g_{LT}(T)\cdot(1-\alpha(T)) + g_{HT}(T)\cdot\alpha(T) \quad (6)$$

where $\alpha(T)$ is the residence probability of the spin triad at HT geometry, and g_{LT} and g_{HT} are the g-factors of the spin triad at the corresponding geometry which have the following dependences on temperature:

$$g_{LT}(T) = \frac{(4g^{R} - g_{LT}^{Cu}) + 3g_{LT}^{Cu}\cdot e^{2J_{LT}/kT} + 10\cdot(2g^{R} + g_{LT}^{Cu})\cdot e^{3J_{LT}/kT}}{3(1 + e^{2J_{LT}/kT} + 10e^{3J_{LT}/kT})} \quad (7)$$

$$g_{HT}(T) = \frac{(4g^{R} - g_{HT}^{Cu}) + 3g_{HT}^{Cu}\cdot e^{2J_{HT}/kT} + 10\cdot(2g^{R} + g_{HT}^{Cu})\cdot e^{3J_{HT}/kT}}{3(1 + e^{2J_{HT}/kT} + 10e^{3J_{HT}/kT})} \quad (8)$$

Here J_{HT} and J_{LT} are constant intracluster copper(II)−nitroxide exchange interaction values in HT and LT geometries, respectively.

Since $|J_{HT}|$ is quite small (ca. 10 cm^{-1}), all multiplets of the spin triad in HT geometry can be considered equally populated at temperatures $kT \gg |J_{HT}|$ and g_{HT} becomes temperature-independent. We assume $|J_{LT}| \gg kT$, so that only the lowest multiplet of the spin triad is populated and g_{LT} is also temperature-independent. This assumption allowed us to calculate $\alpha(T)$ dependences for both compounds (Figure 8a) using $g_{eff}(T)$ measured for single crystals at Q-band (Figure 6).

The $\alpha(T)$ for $Cu(hfac)_2L^{Pr}$ and $Cu(hfac)_2L^{Bu}\cdot 0.5C_8H_{18}$ can be compared with X-ray data shown in Figure 8b. Indeed, the Cu−O_{hfac} and Cu−O_L bond lengths depend on temperature and coincide at certain intermediate temperature. The range of bond length changes is similar for Cu−O_{hfac} and Cu−O_L and the crossing point indicates equal residence probabilities in the high- and low-temperature geometry ($\alpha = 0.5$). The X-ray data yield $T(\alpha = 0.5) \approx 120$ K for $Cu(hfac)_2L^{Bu}\cdot 0.5C_8H_{18}$ and $T(\alpha = 0.5) \approx 200$ K for $Cu(hfac)_2L^{Pr}$. The $T(\alpha = 0.5)$ value agrees well with the $\alpha(T)$ obtained from EPR of $Cu(hfac)_2L^{Bu}\cdot 0.5C_8H_{18}$, whereas for the $Cu(hfac)_2L^{Pr}$ compound $T(\alpha = 0.5) \approx 170$ K (Figure 8a). The observed discrepancy for $Cu(hfac)_2L^{Pr}$ means that $|J_{LT}|$ is not large enough as was assumed. Indeed, if the phase transition extends up to 250 K (the case of $Cu(hfac)_2L^{Pr}$), it is quite reasonable to expect that the upper multiplets of the spin triads at LT geometry are noticeably populated at high temperatures. This can be taken into account considering g_{LT} to be temperature-dependent according to eq 7. Figure 8a (blue circles) shows the $\alpha(T)$ dependence calculated for $J_{LT} = -150$ cm^{-1} that agrees with the X-ray-determined reference $T(\alpha = 0.5) \approx 200$ K. The obtained value $J_{LT} = -150$ cm^{-1} is very reasonable and agrees well with the one determined in model A at low temperatures (Figure 7a). The LT geometry of spin triads in the $Cu(hfac)_2L^{Bu}\cdot 0.5C_8H_{18}$ compound is similar to that of $Cu(hfac)_2L^{Pr}$; therefore, one would expect a similar value of the intracluster exchange interaction $J_{LT} \sim -150$ cm^{-1} for $Cu(hfac)_2L^{Bu}\cdot 0.5C_8H_{18}$.

Physically, the residence probability $\alpha(T)$ (Figure 8a) is determined by Jahn−Teller dynamics between two potential wells corresponding to the HT and LT geometries. A number of studies addressed this problem in the case of copper(II) ions doped into diamagnetic matrices.[49−51] It was noticed that the potential surface may change with temperature due to the temperature dependence of the orthorhombic component of the lattice strain, so that the residence probability is influenced by both the Boltzman factor and changes in the relative depths of the two (HT and LT) potential wells.[52,53] We expect similar trends for breathing crystals as well; however, these more complex highly cooperative polymer-chain complexes cannot yet be described at the same level of theory.

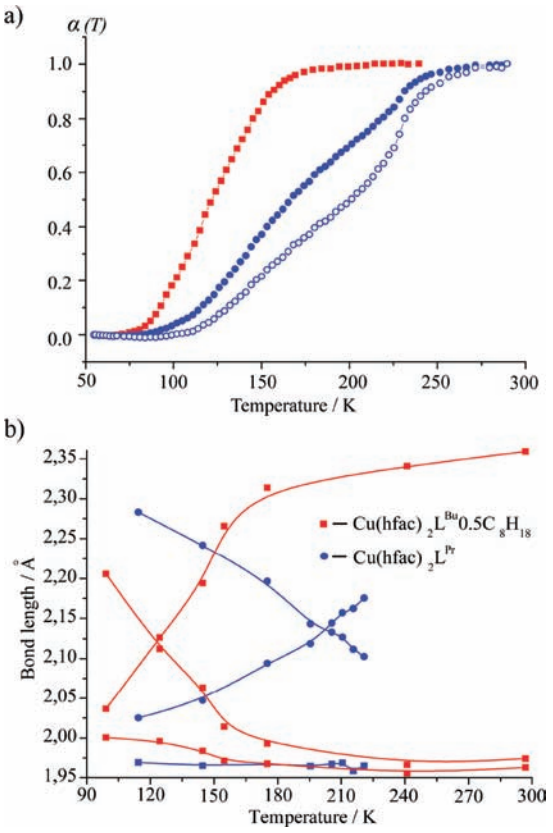

Figure 8. (a) Residence probability of the spin triad in HT geometry $\alpha(T)$ for $Cu(hfac)_2L^{Pr}$ (blue ●) and $Cu(hfac)_2L^{Bu}\cdot 0.5C_8H_{18}$ (red ■) assuming $|J_{LT}| \gg kT$ over the whole temperature range. In the case of $Cu(hfac)_2L^{Pr}$, agreement with X-ray data can be achieved by taking into account $J_{LT} = -150$ cm^{-1} for the LT geometry of the spin triad (blue ○). (b) Temperature-dependent bond length changes for the studied compounds as observed by X-ray crystallography: $Cu(hfac)_2L^{Pr}$ (blue ●) and $Cu(hfac)_2L^{Bu}\cdot 0.5C_8H_{18}$ (red ■). For each compound, Cu−O_{hfac} and Cu−O_L bond lengths, that "cross" with temperature, are shown. Note that the Cu−O_L bond lengths increase with temperature, whereas the Cu−O_{hfac} bond lengths decrease with increasing temperature. The error of bond length determination does not exceed 0.004 Å.

Summarizing, in model B every spin triad at a certain moment of time can be found in one of two stable geometries (LT and HT) that differ by magnetic moment and g-factor, and the fast jumps (10^9 s^{-1} and higher) between these geometries occur in time. The main parameter characterizing the phase transition is the residence probability of the spin triad in each of these geometries, which originates from Jahn−Teller dynamics between HT and LT potential wells. EPR allows one to obtain the temperature dependence of this residence probability $\alpha(T)$, and the analysis of $\alpha(T)$ dependences and X-ray data yields an estimate of the intracluster exchange interaction for the spin triad in the LT geometry.

Model C: Static Spin Triads Coupled by Strong Intercluster Exchange. With the assumption that the dynamic Jahn−Teller

dx.doi.org/10.1021/ic2011869 |*Inorg. Chem.* 2011, 50, 10204–10212

effect (model B) is absent, during the gradual spin transition there is simply a consequent stochastic switching of the CuO_6 units from HT to LT geometry. Then, the gradual curve of the magnetic susceptibility $\mu_{eff}(T)$ simply reflects the temperature-dependent ratio of spin triads in the HT and LT states. If the distribution of one phase (HT/LT) in the other is random, the direct interpretation of the X-ray data will also give an average geometry (in this case spatial average). Since the LT and HT geometries are known, one can calculate the HT/LT ratio depending on temperature.[54] Although X-ray and magnetic susceptibility data in model C yield spatially averaged ratios HT/LT, in the case of EPR one would expect these two phases to be detected separately as two well resolved EPR lines. In contrast, X- and Q-band EPR, whose spectral resolution is sufficient to resolve HT and LT phases with g^C and g^A, respectively, did not allow us to detect these separate signals. The only possibility to average signals of HT and LT phases in the EPR spectrum is to assume rather strong intercluster exchange interaction between neighboring spin triads that would be sufficient for coalescence of individual spectra. In our recent work we have demonstrated that indeed this intercluster exchange in breathing crystals can be strong on the EPR scale and vary from ca. 1 to 10 cm^{-1}.[36] The rates of electron jumps between paramagnetic centers coupled by exchange interaction J are usually estimated as $1/J \sim 30-300$ GHz. This seems to be about sufficient to average EPR lines that are spectrally separated by up to a few wavenumbers. Experimental observations also confirm that intercluster exchange is strong enough to average signals with typical g^C and g^A at EPR frequencies up to 94 GHz. For one of the compounds ($Cu(hfac)_2L^{Bu}\cdot 0.5C_6H_{14}$, C_6H_{14} = hexane), the X-ray data show an alternation of HT and LT states in polymer chains of a crystal at low temperatures; however, EPR cannot resolve these two lines but shows one signal with average g-value instead.[31] Therefore, the presence of strong intercluster exchange interaction can explain the observation of single average EPR line of the HT and LT states in the model of random consequently switched triads during a gradual spin transition. In the framework of this model the measured $g_{eff}(T)$ dependence can be interpreted in terms of eq 6, where $\alpha(T)$ now reflects the temperature-dependent ratio of spin triads in HT geometry to the amount of all spin triads. An estimation of the intracluster exchange interaction for the spin triads in LT geometry is the same as in the previous model.

This model C is in principle capable of describing the experimental data observed using EPR, X-ray, and magnetic susceptibility data. Compared to model B, the weakness of model C is the necessity to assume that the distribution of one phase within the other is sufficiently random and homogeneous. At the same time, in most cases of spin-crossover compounds phase transitions occur in domains;[55] i.e., sufficiently large volumes of one phase appear within the other. If this would be the case in breathing crystals, only the triads located close to the domain walls would manifest effectively averaged g-values due to the intercluster exchange interaction, because those deep inside the domain all have the same geometry and magnetic moment and thus intercluster exchange cannot lead to g-factor averaging as observed in EPR. Consequently, model C can describe the experimental observation in EPR only if the domain size is small enough to allow all spin triads of different domains to interact with each other. Whether this is possible in breathing crystals or not is currently unclear and may be the subject of future structural investigations.

Resuming, at the present stage of this research it is not possible to conclude which of the three proposed models (A−C) is the most relevant to describe the phase transitions in breathing crystals on a molecular level. It is possible that all three types of effects are present to some extent or at certain stages of the phase transition. From a practical point of view, model A is most useful as it allows for the characterization of temperature-dependent exchange interaction in breathing crystals. Even though the obtained $J(T)$ dependence might reflect an effective macroscopic parameter, in most physical situations (time span greater than several nanoseconds, sample size larger than several nanometers) this parameter is observed or measured experimentally. On the other hand, when detailed information on phase transitions on a molecular level is requested, one has to turn to models B and C and discriminate between temporal or spatial averaging. These models can give information either on the fast Jahn−Teller dynamics of the spin triads or on the distribution of phases in breathing crystals depending on temperature.

CONCLUSIONS

In this paper we have studied temperature-dependent intracluster exchange interactions in spin triads of switchable molecular magnets $Cu(hfac)_2L^R$, using EPR techniques. The main experimental EPR parameter of the studied compounds is the effective g-factor of the spin triads which nicely reflects the spin transitions taking place in the $Cu(hfac)_2L^R$ family. Different experimental approaches to explain the EPR measurement and interpret $g_{eff}(T)$ were discussed. Although the $g_{eff}(T)$ function can in principle be measured in powders, the best results are obtained using single crystals properly oriented in the magnetic field. In most cases it is convenient to use Q-band EPR, since spectral resolution at this frequency (34 GHz) is sufficient and the experimental data obtained at higher frequencies would require the use of a more complicated theoretical treatment for the interpretation of the obtained $g_{eff}(T)$ dependence. The origin of the gradual dependences $g_{eff}(T)$ and $J(T)$ in two of the studied complexes can be explained using several models that cannot be distinguished on the basis of the presently available EPR, X-ray, and magnetometry data. The interpretation of the obtained exchange interaction is different in these models, whether it is an exact or effective quantity. However, in any case the developed approaches for studying and interpreting $g_{eff}(T)$ and $J(T)$ dependences are useful and instructive for the characterization of the magnetic properties in the growing family of breathing crystals $Cu(hfac)_2L^R$.

AUTHOR INFORMATION

Corresponding Author

*E-mail: sergey.veber@tomo.nsc.ru.

ACKNOWLEDGMENT

This work was supported by the Russian Foundation for Basic Research (11-03-00158 and 09-03-00091), the RF President's Grant (MK-4268.2010.3), the Grant for the Leading Scientific Schools (NSh-7643.2010.3), Federal Agency for Education (P 1144 and P 2439), and the Max Planck Society.

REFERENCES

(1) Kahn, O. *Molecular Magnetism*; VCH: New York, 1993.

(2) *Molecular Magnetism: From Molecular Assemblies to the Devices*; Coronado, E., Delhaès, P., Gatteschi, D., Miller, J. S., Eds.; Nato ASI

Series, E: Applied Sciences 321; Kluwer Academic Publisher: Dordrecht, The Netherlands, 1996.
(3) *Spin Crossover in Transition Metal Compounds*; Gutlich, P., Goodwin, H. A., Eds.; Topics in Current Chemistry 233−235; Springer-Verlag: Berlin, 2004; Vols I−III.
(4) *Magnetism: Molecules to Materials I: Models and Experiments and Magnetism: Molecules to Material II: Molecule-Based Materials and Experiments*; Miller, J. S., Drillon, M., Eds.; Wiley-VCH: New York, 2001.
(5) *Molecular Magnets: Recent Highlights*; Linert, W., Verdaguer, M., Eds.; Springer-Verlag: Wien, Austria, 2003.
(6) Carbonera, C.; Dei, A.; Letard, J. F.; Sangregorio, C.; Sorace, L. *Angew. Chem., Int. Ed.* **2004**, *43*, 3136–3138.
(7) Dei, A.; Poneti, G.; Sorace, L. *Inorg. Chem.* **2010**, *49*, 3271–3277.
(8) Niel, V.; Thompson, A. L.; Goeta, A. E.; Enachescu, C.; Hauser, A.; Galet, A.; Munoz, M. C.; Real, J. A. *Chem.—Eur. J.* **2005**, *11*, 2047–2060.
(9) Enachescu, C.; Linares, J.; Varret, F.; Boukheddaden, K.; Codjovi, E.; Salunke, S. G.; Mukherjee, R. *Inorg. Chem.* **2004**, *43*, 4880–4888.
(10) Real, J. A.; Andres, E.; Munoz, M. C.; Julve, M.; Granier, T.; Bousseksou, A.; Varret, F. *Science* **1995**, *268*, 265–267.
(11) Clemente-Juan, J. M.; Mackiewicz, C.; Verelst, M.; Dahan, F.; Bousseksou, A.; Sanakis, Y.; Tuchagues, J. P. *Inorg. Chem.* **2002**, *41*, 1478–1491.
(12) Bousseksou, A.; Molnar, G.; Matouzenko, G. *Eur. J. Inorg. Chem.* **2004**, *22*, 4353–4369.
(13) Sato, O.; Tao, J.; Zhang, Y. Z. *Angew. Chem., Int. Ed.* **2007**, *46*, 2152–2187.
(14) Dei, A.; Gatteschi, D.; Sangregorio, C.; Sorace, L. *Acc. Chem. Res.* **2004**, *37*, 827–835.
(15) Ovcharenko, V. I.; Fokin, S. V.; Romanenko, G. V.; Shvedenkov, Yu. G.; Ikorskii, V. N.; Tretyakov, E. V.; Vasilevskii, S. F. *Zh. Strukt. Khim.* **2002**, *43*, 163. *Russ. J. Struct. Chem.* **2002**, *43*, 153 (English Translation).
(16) Rey, P.; Ovcharenko, V. I. Copper(II) Nitroxide Molecule Spin-Transition Complexes. In *Magnetism: Molecules to Materials IV*; Miller, J. S., Drillon, M., Eds.; Wiley-VCH: New York, 2003; pp 41−63.
(17) Ovcharenko, V. I.; Fokin, S. V.; Romanenko, G. V.; Ikorskii, V. N.; Tretyakov, E. V.; Vasilevskii, S. F.; Sagdeev, R. Z. *Mol. Phys.* **2002**, *100*, 1107–1115.
(18) Ovcharenko, V. I.; Maryunina, K. Yu.; Fokin, S. V.; Tretyakov, E. V.; Romanenko, G. V.; Ikorskii, V. N. *Russ. Chem. Bull. Int. Ed.* **2004**, *53*, 2406–2427.
(19) Ovcharenko, V. I.; Romanenko, G. V.; Maryunina, K. Yu.; Bogomyakov, A. S.; Gorelik, E. V. *Inorg. Chem.* **2008**, *47*, 9537–9552.
(20) Ovcharenko, V. I. In *Stable Radicals: Fundamentals and Applied Aspects of Odd-Electron Compounds*; Hicks, R., Ed.; Wiley-VCH: New York, 2010; pp 461−506.
(21) Romanenko, G. V.; Maryunina, K. Y.; Bogomyakov, A. S.; Sagdeev, R. Z.; Ovcharenko, V. I. *Inorg. Chem.* **2011**, *50*, 6597–6609.
(22) Iwahori, F.; Inoue, K.; Iwamura, H. *Mol. Cryst. Liq. Cryst. Sci. Technol., Sect. A* **1999**, *334*, 533–538.
(23) Okazawa, A.; Ishida, T. *Inorg. Chem.* **2010**, *49*, 10144–10147.
(24) Okazawa, A.; Hashizume, D.; Ishida, T. *J. Am. Chem. Soc.* **2010**, *132*, 11516–11524.
(25) Baskett, M.; Lahti, P. M.; Paduan-Filho, A.; Oliveira, N. F. *Inorg. Chem.* **2005**, *44*, 6725–6735.
(26) dePanthou, F. L.; Belorizky, E.; Calemczuk, R.; Luneau, D.; Marcenat, C.; Ressouche, E.; Turek, P.; Rey, P. *J. Am. Chem. Soc.* **1995**, *117*, 11247–11253.
(27) dePanthou, F. L.; Luneau, D.; Musin, R.; Ohrstrom, L.; Grand, A.; Turek, P.; Rey, P. *Inorg. Chem.* **1996**, *35*, 3484–3491.
(28) Caneschi, A.; Chiesi, P.; David, L.; Ferraro, F.; Gatteschi, D.; Sessoli, R. *Inorg. Chem.* **1993**, *32*, 1445–1453.
(29) Fedin, M.; Veber, S.; Gromov, I.; Ovcharenko, V.; Sagdeev, R.; Schweiger, A.; Bagryanskaya, E. *J. Phys. Chem. A* **2006**, *110*, 2315–2317.
(30) Fedin, M.; Veber, S.; Gromov, I.; Ovcharenko, V.; Sagdeev, R.; Bagryanskaya, E. *J. Phys. Chem. A* **2007**, *111*, 4449–4455.
(31) Fedin, M.; Veber, S.; Gromov, I.; Maryunina, K.; Fokin, S.; Romanenko, G.; Sagdeev, R.; Ovcharenko, V.; Bagryanskaya, E. *Inorg. Chem.* **2007**, *46*, 11405–11415.
(32) Veber, S. L.; Fedin, M. V.; Potapov, A. I.; Maryunina, K. Yu.; Romanenko, G. V.; Sagdeev, R. Z.; Ovcharenko, V. I.; Goldfarb, D.; Bagryanskaya, E. G. *J. Am. Chem. Soc.* **2008**, *130*, 2444–2445.
(33) Fedin, M.; Ovcharenko, V.; Sagdeev, R.; Reijerse, E.; Lubitz, W.; Bagryanskaya, E. *Angew. Chem., Int. Ed.* **2008**, *47*, 6897–6899. *Angew. Chem.* **2008**, *120*, 7003–7005.
(34) Veber, S. L.; Fedin, M. V.; Maryunina, K. Yu.; Romanenko, G. V.; Sagdeev, R. Z.; Bagryanskaya, E. G.; Ovcharenko, V. I. *Inorg. Chim. Acta* **2008**, *361*, 4148–4152.
(35) Fedin, M. V.; Veber, S. L.; Romanenko, G. V.; Ovcharenko, V. I.; Sagdeev, R. Z.; Klihm, G.; Reijerse, E.; Lubitz, W.; Bagryanskaya, E. G. *Phys. Chem. Chem. Phys.* **2009**, *11*, 6654–6663.
(36) Fedin, M. V.; Veber, S. L.; Maryunina, K. Yu.; Romanenko, G. V.; Suturina, E. A.; Gritsan, N. P.; Sagdeev, R. Z.; Ovcharenko, V. I.; Bagryanskaya, E. G. *J. Am. Chem. Soc.* **2010**, *132*, 13886–13891.
(37) Fedin, M. V.; Veber, S. L.; Sagdeev, R. Z.; Ovcharenko, V. I.; Bagryanskaya, E. G. *Russ. Chem. Bull., Int. Ed.* **2010**, *59*, 1065–1079.
(38) Masters, V. M.; Riley, M. J.; Hitchman, M. A. *J. Synchrotron Radiat.* **1999**, *6*, 242–243.
(39) Goldfarb, D.; Lipkin, Ya.; Potapov, A.; Gorodetsky, Y.; Epel, B.; Raitsimring, A. M.; Radoul, M.; Kaminker, I. *J. Magn. Reson.* **2008**, *194*, 8–15.
(40) Musin, R. N.; Schastnev, P. V.; Malinovskaya, S. A. *Inorg. Chem.* **1992**, *31*, 4118–4121.
(41) Vancoillie, S.; Rulisek, L.; Neese, F.; Pierloot, K. *J. Phys. Chem. A* **2009**, *113*, 6149–6157.
(42) Benelli, C.; Gatteschi, D.; Zanchini, C.; Latour, J. M.; Rey, P. *Inorg. Chem.* **1986**, *25*, 4242–4244.
(43) Ginsberg, A. P.; Lines, M. E. *Inorg. Chem.* **1972**, *11*, 2289.
(44) Hathaway, B. *Struct. Bonding (Berlin)* **1984**, *57*, 55–118.
(45) Reinen, D.; Atanasov, M. *Chem. Phys.* **1991**, *155*, 157–171.
(46) Bersuker, I. B. *Electronic Structure and Properties of Transition Metal Compounds*; Wiley-Interscience: New York, 1996.
(47) Simmons, C. J.; Stratemeier, H.; Hanson, G. R.; Hitchman, M. A. *Inorg. Chem.* **2005**, *44*, 2753–2760.
(48) Hoffmann, S. K.; Goslar, J. *Acta Phys. Pol., A* **2006**, *110*, 807–816.
(49) Silver, B. L.; Getz, D. *J. Chem. Phys.* **1974**, *61*, 638–650.
(50) Bebendorf, J.; Bürgi, H. B.; Gamp, E.; Hitchman, M. A.; Murphy, A.; Reinen, D.; Riley, M. J.; Stratemeier, H. *Inorg. Chem.* **1996**, *35*, 7419–7429.
(51) Riley, M. J.; Hitchman, M. A.; wan Mohammed, A. *J. Chem. Phys.* **1987**, *87*, 3766–3778.
(52) Hitchman, M. A.; Maaskant, W.; van der Plas, J.; Simmons, C. J.; Stratemeier, H. *J. Am. Chem. Soc.* **1999**, *121*, 1488.
(53) Augustyniak, M. A.; Krupski, M. *Chem. Phys. Lett.* **1999**, *311*, 126.
(54) Zueva, E. M.; Ryabykh, E. R.; Kuznetsov, A. M. *Russ. Chem. Bull.* **2009**, *58*, 1654–1662.
(55) Sorai, M. *Top. Curr. Chem.* **2004**, *235*, 153–170.